# Searching for Supersymmetry with the $\alpha_T$ variable in $p\bar{p}$ collisions with the CMS Detector at the Large Hadron Collider

*Zoe Hatherell*

A thesis submitted in fulfilment of the requirements
for the degree of Doctor of Philosophy
to Imperial College London
December 2011

# Contents

# Chapter 1

# Searching for Supersymmetry with $\alpha_T$ in all-hadronic events

The analysis presented here represents a model-independent search for new physics in the all-hadronic channel, where the final state is defined by the presence of jets and missing energy. Designed to search for signs of supersymmetry whilst remaining sensitive to other new physics models, an inclusive strategy is used imposing restrictions only on the final state. Events are chosen based on their compatibility with a topology of heavy new particles pair-produced in p-p collisions, which decay through a chain with an end product which is stable and undetectable.

Isolating these new physics events from Standard Model background processes is essential in order to identify an excess. Controlling the dominant background from QCD Multijet processed is the central feature of the strategy, implementing use of the powerful discriminant, the $\alpha_{\mathrm{T}}$ variable described in Chapter **??**. The remaining backgrounds from electroweak processes may then be accounted for using data-driven estimation techniques in muon and photon control samples.

## 1.1 Samples

This analysis uses datasets both from Monte Carlo simulation (MC) and of data recorded by the CMS detector in 2011.

### 1.1.1 Monte Carlo Simulation

Datasets of simulated events with calculated cross-sections are required for any analysis at the LHC. Due to the hadron-collider nature these rely on the PDF's

#### Standard Model Background

#### CMSSM SUSY Signal

For the purpose of understanding the possible yields from CMSSM SUSY, two mSUGRA parameter points are used. CMS has a dedicated set of 10 Low Mass(LM) points designed for initial data-taking from which we have chosen LM4 and LM6, the values of which are found in Table 1.1.

| **mSUGRA Point** | $m_0$ | $m_{1/2}$ | $A_0$ | $\tan\beta$ | sign($\mu$) |
|---|---|---|---|---|---|
| **LM4** | 210 GeV | 285 GeV | 0 | 10 | + |
| **LM6** | 85 GeV | 400 GeV | 0 | 10 | + |

*Table 1.1: The two CMSSM SUSY signal points used and their corresponding mSUGRA parameter values.*

These points are chosen for their existence above the exclusion limit set previously, shown in Figure 1.1 on the exclusion plot from the 2010 iteration of this analysis[2].

The

### 1.1.2 Data Sample

This analysis considers data collected by CMS at $\sqrt{s} = 7$ TeV in 2011 between March and June, during the data-taking period known locally as Run2011A. Analyses use only the data taken whilst CMS was fully operational, and thus the data used were specified by the certified list of "good runs" that correspond to $1.1 fb^{-1}$ of integrated luminosity.

As described previously, loose requirements on the types of triggers passed allow the sorting of the data into each Primary Dataset (PD). For the hadronic analysis the HT dataset is used, with basic low-threshold $H_T$ triggers required. Higher threshold triggers are applied subsequently as part of the analysis selection, detailed in Section 1.2.

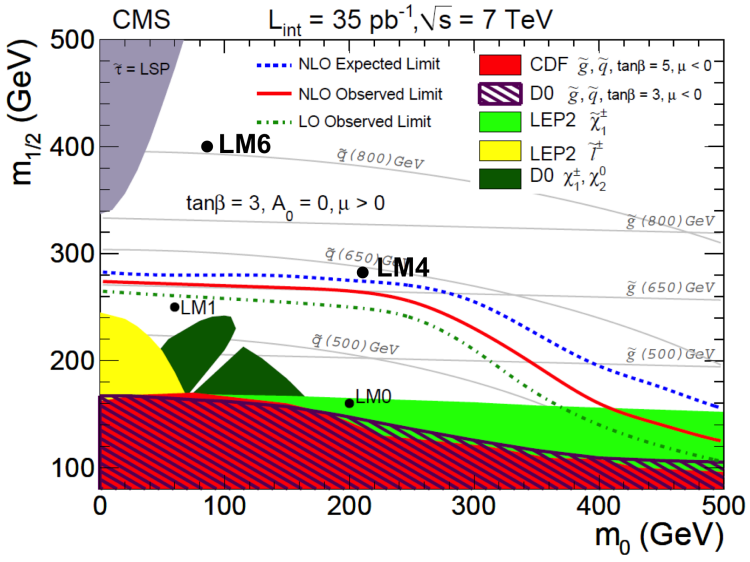


*Figure 1.1: The exclusion limit set in the previous incarnation of this analysis with the 35pb$^{-1}$ 2010 CMS dataset shown in the $m_0 - m_{1/2}$ plane with tan $\beta$ = 10, $A_0 = 0$ and sign($\mu$) = +. Reference points LM4 and LM6 to be used in the 2011 analysis are illustrated, in the region yet to be excluded. Previously used reference points LM0 and LM1 are shown below the limit already excluded [2].*

For the data-driven estimation techniques muon and photon control samples are defined. For the muon control sample, the HT PD is also used, as a low muon $p_T$ requirement makes this better suited than the dedicated Muon PD. However the photon control sample uses the dedicated Photon PD that requires some basic threshold photon triggers to be passed.

## 1.2 Trigger

In order to select the signal events and minimise the contamination from backgrounds, a set of selection criteria is applied. As described previously in Section , data collected by the CMS detector is stored and organised according to the L1 and HLT trigger paths passed. Each given dataset then undergoes the offline event reconstruction described in Chapter RECON/IDEN, after which n-tuples are constructed from which we apply cuts on objects and analysis variables.

Previous incarnations of this analysis for the 2010 dataset REFF used a set of pure $H_T$triggers, however these are unsuitable for the 2011 analysis as these have too high thresholds for the analysis due to the increase in instantaneous

luminosity. The use of cross-object triggers is now employed, requiring events that pass thresholds in both $H_T$and $\not{H}_{\mathrm{T}}$ for the signal region, and using the lowest un-prescaled thresholds available to ensure signal yields are accurate.

As this analysis makes use of those events which fail the selection criteria also, the hadronic control sample, the pre-scaled $H_T$triggers are still used taking into account the pre-scaled factors. In the muon control sample, due to the low $p_{\mathrm{T}}$threshold we use the same triggers as for the hadronic signal sample, and the photon sample makes use of the single photon trigger paths.

Having passed one of the un-prescaled triggers the events are subjected to a series of cuts on objects and analysis variables in order to select the event topologies required and minimise the background contamination.

## 1.3 Object Definitions

### 1.3.1 Jets

The jets used in this analysis are Calo Jets, reconstructed as described in Section **??** using the anti-k$_T$ jet clustering algorithm. In addition, a reconstructed jet must pass an additional selection in order to be considered for the analysis:

- Corrected jet transverse momentum requirement of $p_{\mathrm{T}}> 50$ GeV
- Jet pseudo-rapidity $|\eta| < 3$ required to ensure within the fiducial range of the calorimeter systems.
- Passes"loose" jet identification criteria to reject jets resulting from unphysical energy using cuts in Table 1.2.

Any jet which pass the $E_{\mathrm{T}}$ and $\eta$ requirements but fails the "loose" identification criteria is noted, and the event is marked as containing an "odd" jet, as the presence of such a particle reflects an event whose kinematics are poorly understood and may therefore lead to a misleading $\not{H}_{\mathrm{T}}$.

### 1.3.2 Muons

Although muons are not required by the analysis, a veto on them must be employed, based on muons that satisfy the following set of criteria:

| Definition | Variable | ID Cut |
|---|---|---|
| Fraction of jet energy contributed by the "hottest" hybrid photo-diode | $f_{HPD}$ | $< 0.98$ |
| Minimum number of cells required to contribute 90% of the jet energy | $N^{90}_{cells}$ | $\leq 2$ |
| Fraction of jet energy contributed by deposits in ECAL | $f_{EM}$ | $> 0.01$ |
| Balance of the energy measured in the short($E_S$) and long($E_L$) HF fibers. | $R_{HF} = \frac{(E_S - E_L)}{(E_S + E_L)}$ (if $p_T^{jet} > 80$ GeV) | $R_{HF} > -0.9$ ($-0.9 < R_{HF} < 1$) |

*Table 1.2: Set of cuts applied in "loose" CaloJet ID used to reject jets resulting from fake calorimeter deposits representing unphysical energy. Devised using cosmic run data as a pure sample of non-collider "fake" jets, full details of which can be found in [1]*

- $p_{\mathrm{T}}{}^{\mu} > 10$ GeV
- $|\eta| < 2.5$
- Relative Combined Isolation = $(Iso_{tracker} + Iso_{ECAL} + Iso_{HCAL})/p_T^{\mu} < 0.15$[1]
- Passes "tight" muon identification, using cuts shown in Table 1.3.

| Definition | Variable | ID Cut |
|---|---|---|
| Reconstructed with outside-in algorithm | Global Muon | Required |
| Reconstructed with inside-out algortithm | Tracker Muon | Required |
| Global muon track fit quality | $\chi^2$ | $< 10$ |
| Number of hits in the silicon tracker included in track | $N_{trk\ hits}$ | $> 10$ |
| Transverse impact parameter with respect to vertex | $d_{xy}$ | $<2$ mm |

*Table 1.3: Set of cuts applied in "tight" Muon ID*

[1]The components $Iso_{tracker}(Iso_{ECAL}, Iso_{HCAL})$ represent the sum of $p_{\mathrm{T}}(E_T)$ in the relevant detector component, calculated in a cone of R = 0.3 in $\eta - \phi$ around there muon trajectory. The track hits used to reconstruct the muon are not used and any muon deposit in the calorimeters is removed via a smaller veto cone.

### 1.3.3 Electrons

### 1.3.4 Photons

sat

## 1.4 Pre-Selection

The events selected must be identified as good events from the CMS detector, using a pre-selection. It is required that events have at least one good primary vertex that is not fake, with $N_{dof}$ ¿ 4 and a vertex position along he beam axis of —$z_{vtx}$— < 24 cm and perpendicular to the axis of $\rho$ ¡ 2 cm. Events that have many fake tracks are identified as monester events and removed, by requiring that the ratio of High Purity tracks to the total number be greater than 25% in events with more than 9 tracks.

Events where noise has been identified in the HCAL are removed also, using an algorithm which checks for Photodetectors which have at east 17 out of 18 channels with an E ¿ 1.5 GeV.

Events are then selected according to the following preselection:

- Require events with $\mathrm{N}_{jet} \geq 2$
- $\mathrm{N}_{muon}$, $\mathrm{N}_{electron}$, $\mathrm{N}_{photon} = 0$ where $p_{\mathrm{T}\mu,e} \geq 10$ GeV, $p_{\mathrm{T}\gamma} \geq 25$ GeV
- $H_T \geq$ 275 GeV
- To protect the quantity $\alpha_{\mathrm{T}}$ from the scenario where many jets exist below the momentum acceptance threshold, the missing energy variable $\not{H}_{\mathrm{T}}$ estimated from jet measurment is compared to the quantity $\not{E}_{\mathrm{T}}$ measured from the calorimters. If the ratio $\mathrm{R}_{miss} = \not{H}_{\mathrm{T}}/\not{E}_{\mathrm{T}} > 1.25$, the event is rejected.

## 1.5 An $H_T$ Shape Analysis

Previous iterations of this analysis strategy with the 35pb$^{-1}$ 2010 LHC dataset [2] used a cut-and-count strategy for all events passing the selection, defining the signal region by an $H_T > 375$ and using lower regions in $H_T$as control regions.

The 2011 analysis follows the same selection but motivated by the increasing luminosity is undertaken as a Shape Analysis in bins of $H_T$, using the whole range $H_T$ >275 GeV as a signal region. This allows greater sensitivity to states of higher mass.

The set of lower bin edges are as follows: [275,325,375,475,574,675,775,875], where each bin is exclusive with an upper limit corresponding to the lower edge of the next bin, except in the case of the final bin which is inclusive $H_T$ >875. The background estimation techniques employed from data therefore are designed to identify the contribution in each distinct bin.

In order to include the two lowest bins in $H_T$is is necessary to scale the jet thresholds stated in Section **??** in order to maintain even event kinematics allowing a shape analysis approach. The background from $t\bar{t}$ + jets carries a bias to higher jet multiplicities compared to the other EWK components, and thus with identical jet definitions exhibits a turn on behaviour in $H_T$. In order to remedy this, the lowest two bins have the two jet energy requirements scaled by $^{l}/_{375.}$ where $l$ represents the bin lower edge in question.

## 1.6 Data to Monte-Carlo Comparisons

### 1.6.1 Dependence of $R_{\alpha_T}$ on $H_T$

## 1.7 Data-Driven Background Estimation

### 1.7.1 Total background prediction

### 1.7.2 Estimating EWK background using high $p_T$ using W+Jets events

**Types of decay contributing to Muon Control Sample**

### 1.7.3 Estimation Z $\nu\bar{\nu}$ + jets background using photon + jets events

## 1.8 Systematic Uncertainties

## 1.9 Simultaneous Fit

## 1.10 Limits

## 1.11 Conclusion

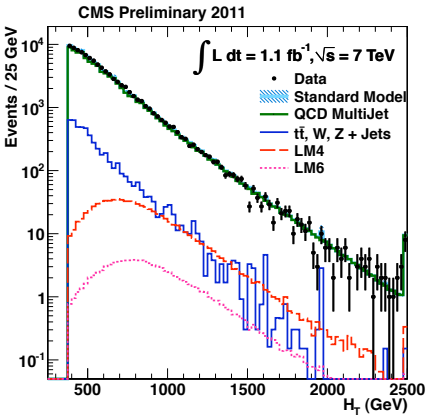


(a) Comparison of $H_T$ between data and MC for the hadronic selection for $H_T \geq 375$ GeV and MHT $> 100$ GeV.

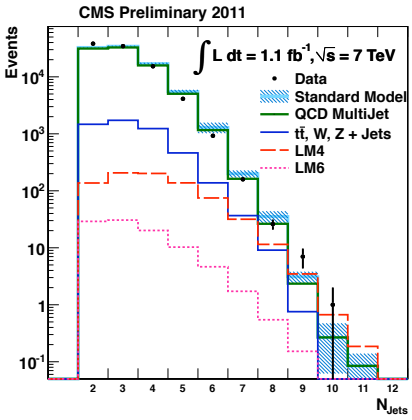


(b) Comparison of the jet multiplicity between data and MC for the hadronic selection, for $H_T \geq 375$ GeV and MHT $> 100$ GeV.

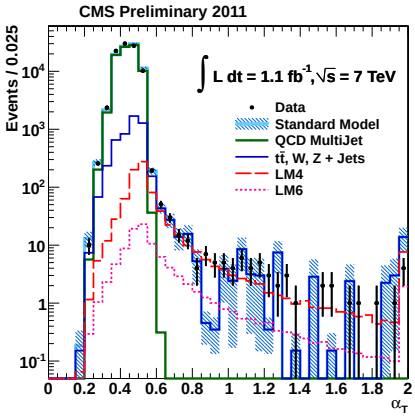


(c) Comparison of the $\alpha_T$ distribution between data and MC for the hadronic selection, for $H_T \geq 375$ GeV and MHT $> 100$ GeV.

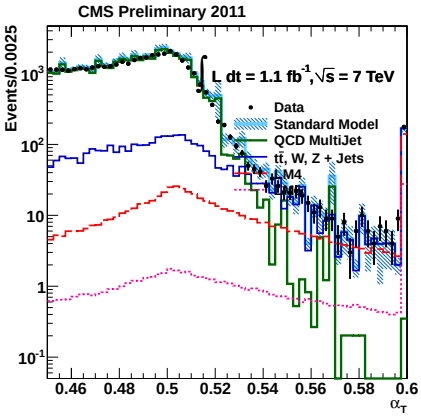


(d) Comparison of the $\alpha_T$ distribution highlighting the agreement on the sharply falling edge between Data and Monte Carlo for the hadronic selection, in the region $H_T \geq 375$ GeV.

*Figure 1.2: Comparisons of 1.1 $fb^{-1}$ 2011 7TeV CMS Data and equivalently weighted Monte-Carlo in basic kinematic quantities prior to the $\alpha_T$ selection cut.*

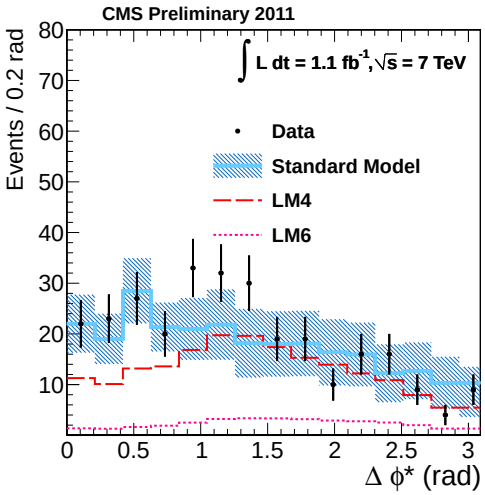


(a) $\Delta\Phi^*$ distribution after $\alpha_T$ selection.

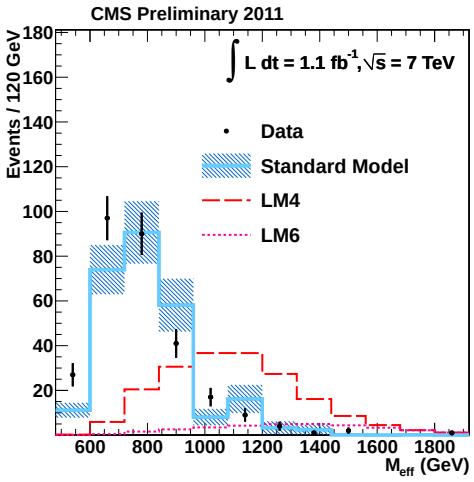


(b) The effective mass distribution, $M_{\text{eff}} = H_T + \text{MHT}$, of the events passing the $\alpha_T$ selection.

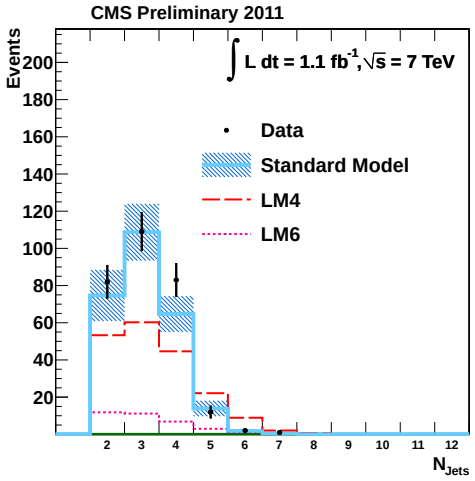


(c) Jet multiplicity after $\alpha_T$ selection.

*Figure 1.3: Comparisons of 1.1 $fb^{-1}$ 2011 7TeV CMS Data and equivalently weighted Monte-Carlo in basic kinematic quantities after the $\alpha_T$ selection cut.*

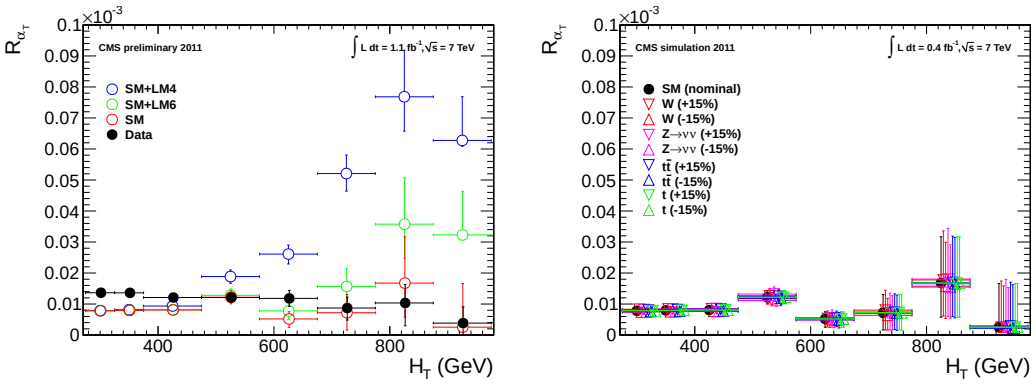


*Figure 1.4: (Left) The dependence of $R_{\alpha_T}$ on $H_T$ for events with $N_{\text{jet}} \geq 2$. (Right) Dependence of rat on $H_T$ when varying the effective cross-section of the four major EWK background components individually by ±15%. (Markers are artificially offset for clarity.)*

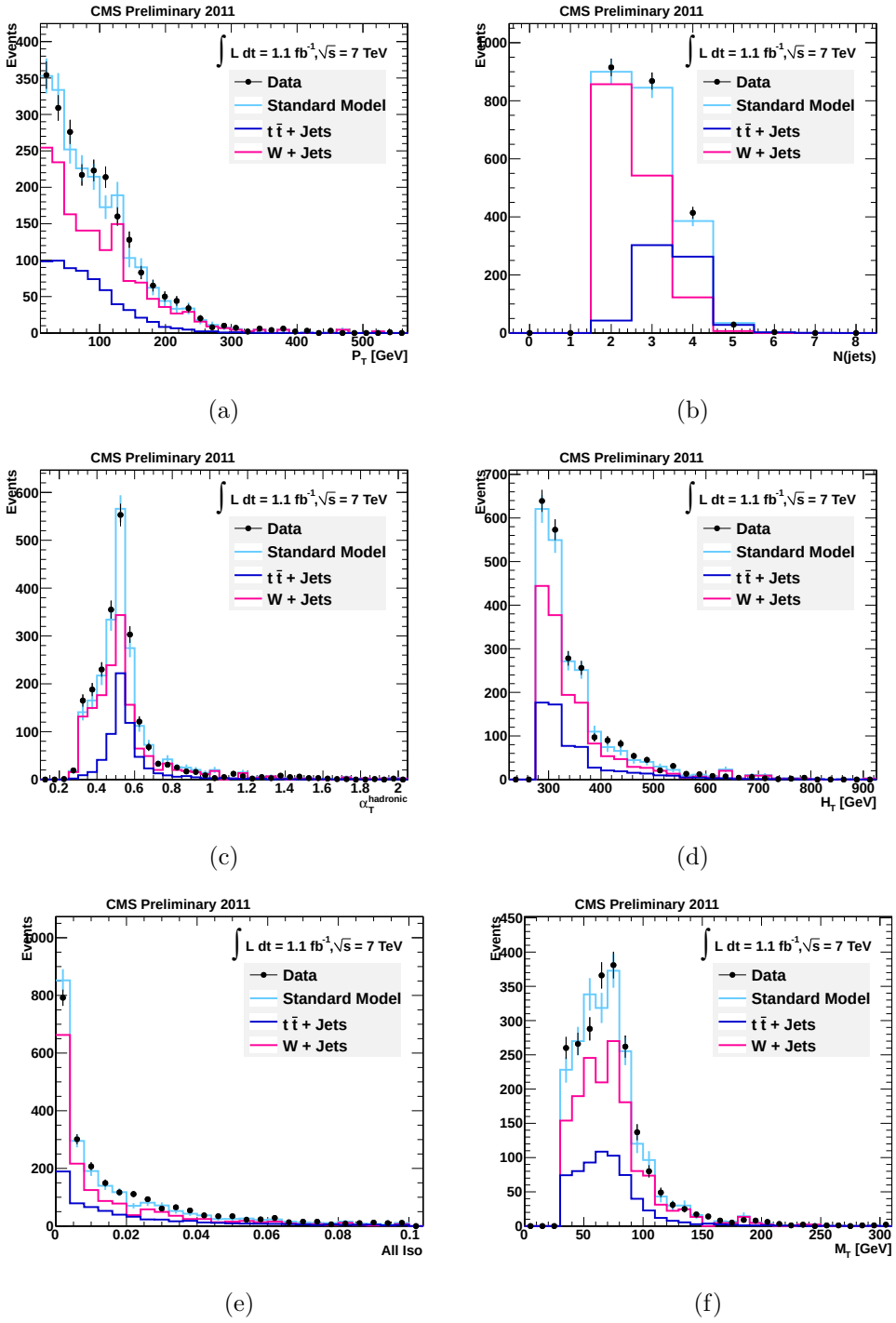


*Figure 1.5: Data - Monte Carlo comparisons for the muon control selection before the $\alpha_T > 0.55$ cut is applied, shown for (a) $\alpha_T$ and (b) $H_T$, (c) Muon Combined Isolation and (d) $M_T$. A cut of* HT *>375 GeV has been applied, to select the region of fixed jet thresholds.*

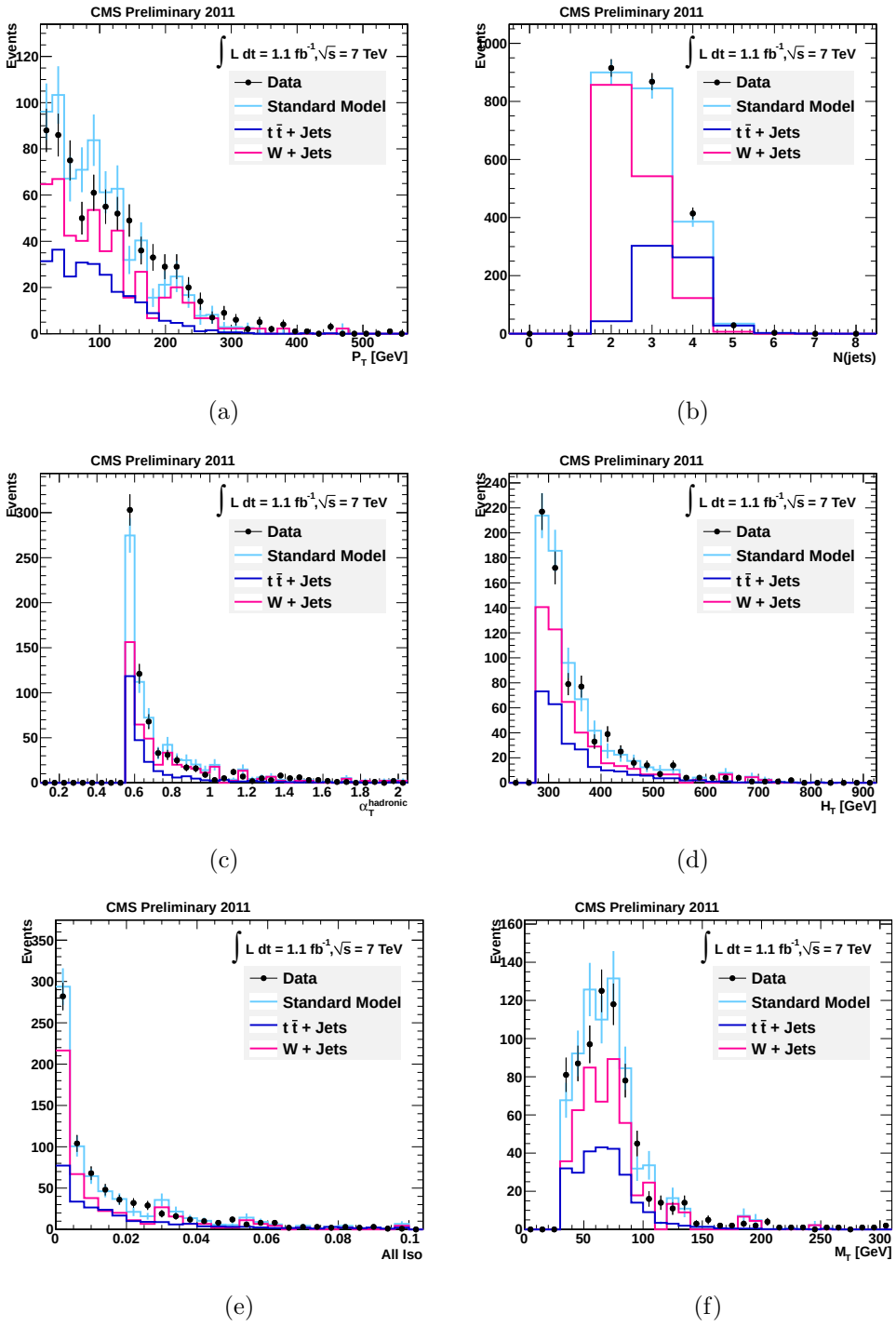


*Figure 1.6: Data - Monte Carlo comparisons for the muon control selection after the $\alpha_T > 0.55$ cut is applied, shown for (a) $H_T$ and (b) $M_T$, (c) Muon Combined Isolation and (d) $M_T$. A cut of* HT *>375 GeV has been applied, to select the region of fixed jet thresholds.*

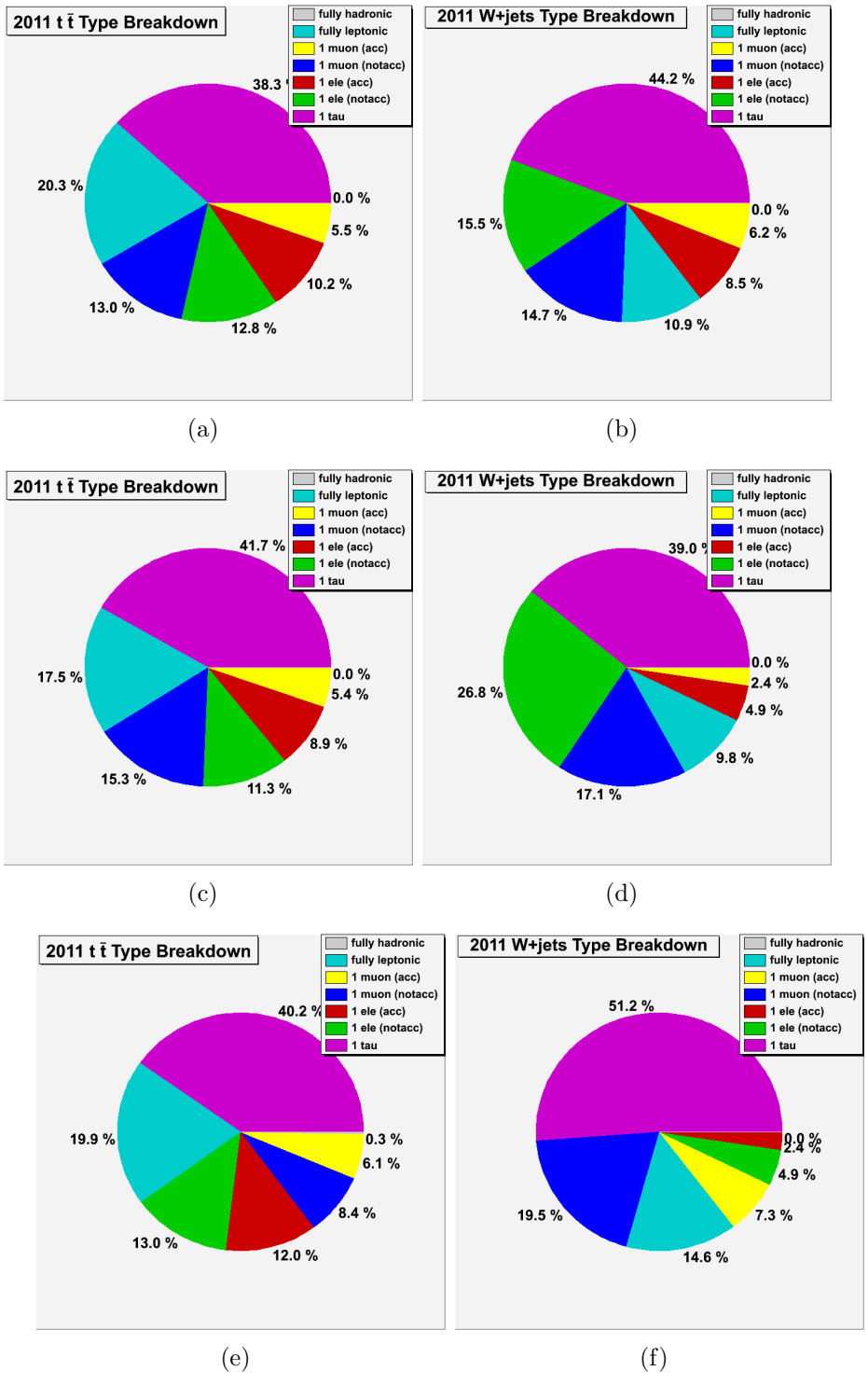


*Figure 1.7: Type breakdown of decays resulting in an event selected by the Muon Control selection, shown using Monte-Carlo truth information separately for* $\mathrm{t\bar{t}}+$ jets *(left) and* $\mathrm{W}+$ jets *(right) events. The breakdown is made separately for each jet-scale case: 275 <$H_T$<325 GeV (top), 325 <$H_T$<375 GeV (middle), and $H_T$>375 GeV (bottom).*

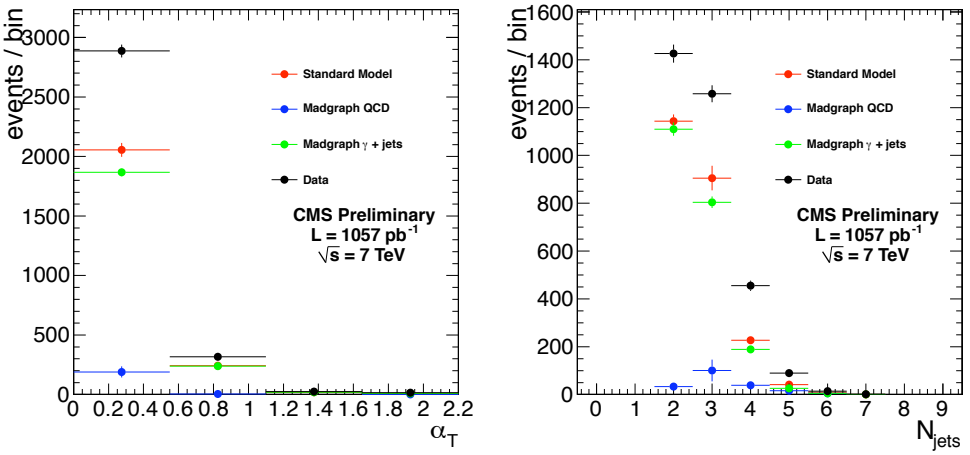


(a) (b)

*Figure 1.8: Data-MC comparisons for the photon control sample. $H_T > 375$ GeV and $\not{H}_T/H_T > 0.4$ are required. Left: the distribution of $\alpha_T$. Right: the distribution of the number of jets.*

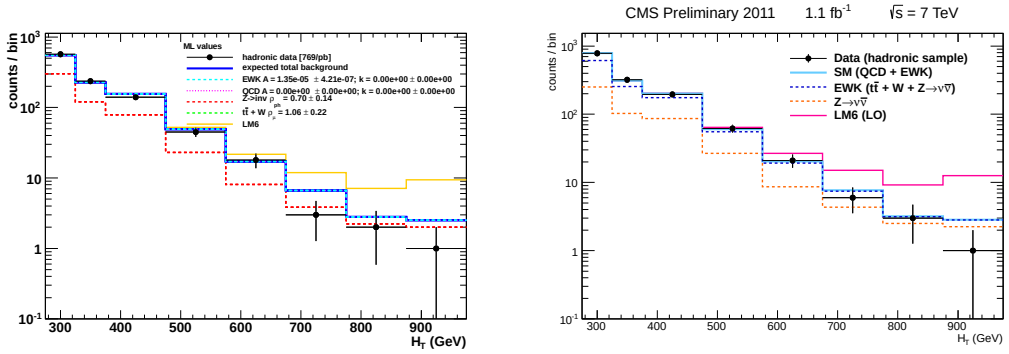


*Figure 1.9: $H_T$ distribution for events in the hadronic signal sample for scenario a) (left) and scenario b) (right). Shown are the events observed in data (black points), the outcome of the fit (blue line) and a breakdown of the individual background contributions as predicted by the control samples. A possible signal contribution from benchmark point LM6 is indicated as well (yellow line).*

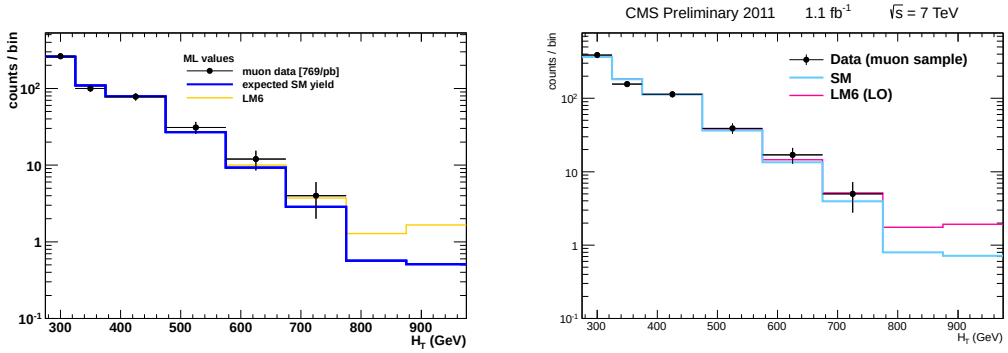


*Figure 1.10: $H_T$ distribution for events selected in the muon control sample for scenario a) (left) and scenario b) (right). Shown are the events observed in data (black points), the outcome of the fit (blue line) and the MC expectation (dashed line). A possible signal contribution from benchmark point LM6 is indicated as well (yellow line).*

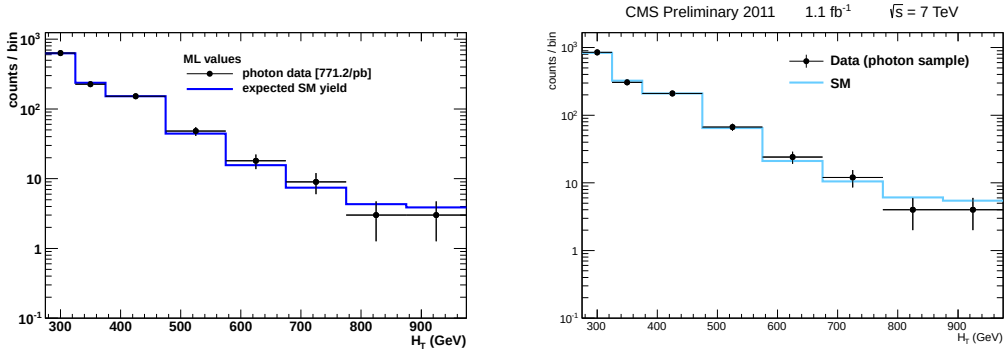


*Figure 1.11: $H_T$ distribution for events selected in the photon control sample for scenario a) (left) and scenario b) (right). Shown are the events observed in data (black points), the outcome of the fit (blue line) and the MC expectation (dashed line).*

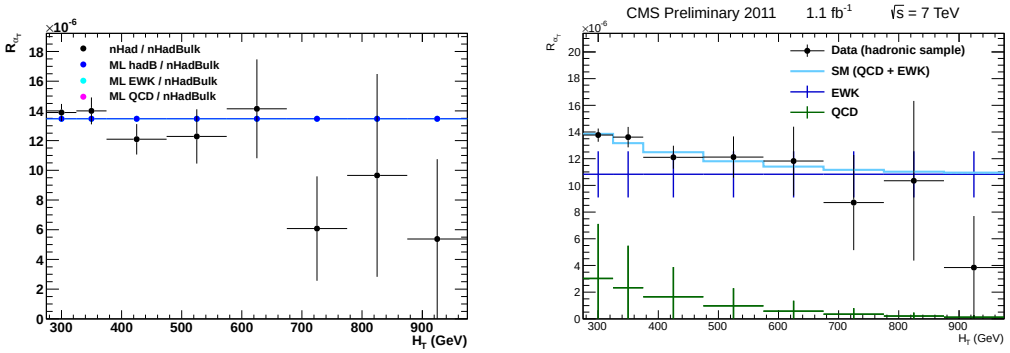


*Figure 1.12: $R_{\alpha_T}$ as a function of $H_T$ as observed in data (black points) and the results of the fit assuming different scenarios: a) (left) and b) (right) .*

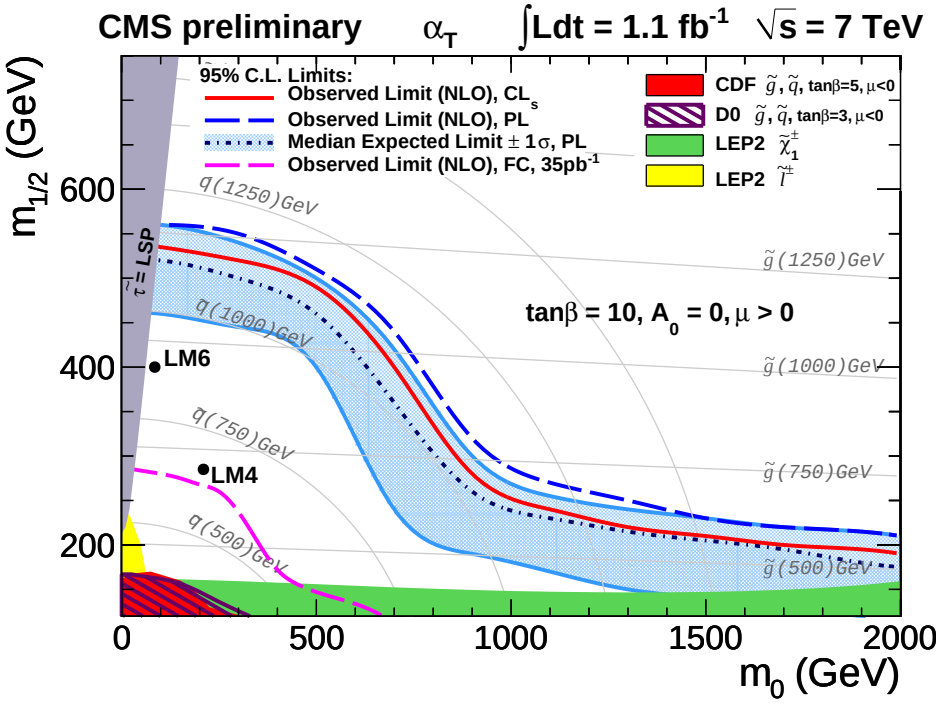


*Figure 1.13: Observed and expected 95% CL exclusion contours in the CMSSM $(m_0, m_{1/2})$ plane $(\tan\beta = 10, A_0 = 0, \mu > 0)$ using NLO signal cross sections using the Profile Likelihood (PL) method. The expected limit is shown with its 68% CL range. The observed limit using the $CL_s$ method is shown as well.*

# Bibliography

[1] The CMS Collaboration. "Calorimeter Jet Quality Criteria for the First CMS Collision Data". **CMS-PAS-JME-09-008**.

[2] Vardan Khachatryan et al. "Search for Supersymmetry in pp Collisions at 7 TeV in Events with Jets and Missing Transverse Energy". *Phys.Lett.*, **B698** (2011) 196–218, 1101.1628.